**Proceedings of the ASME 2021 40th International Conference on Ocean, Offshore and Arctic Engineering**
**OMAE2021**
**June 21-30, 2021, Virtual, Online**

# OMAE2021-62472

## EFFECT OF THE SIMPLIFIED SUPERSTRUCTURE AND SOIL-STRUCTURE INTERACTION MODELS ON THE NATURAL FREQUENCIES OF AN OFFSHORE WIND TURBINE

**Philip Alkhoury[1], Abdul-Hamid Soubra[1], Valentine Rey[1], Mourad Aït-Ahmed[1]**

[1]University of Nantes, France
Correspondence: Philip Alkhoury; Email: Philip.Alkhoury@etu.univ-nantes.fr

## ABSTRACT

*Monopile-supported offshore wind turbines (OWTs) are dynamically sensitive structures, in which their design is principally based on a dimensioning criterion related to its fundamental frequencies. Therefore, an accurate estimation of the natural frequency is essential to assess the working lifetime of the OWT.*

*For the calculation of the OWT natural frequency, several studies exist but few of them simultaneously consider both the real geometrical configuration of the OWT superstructure (blades, nacelle, tower, and transition piece) and the three-dimensional (3D) soil domain and its interaction with the foundation. The aim of this paper is to investigate the suitability of (i) the different simplifying assumptions used in literature for the superstructure and (ii) the recently proposed PISA soil-foundation interaction model, when calculating the natural frequency. This is performed by comparing the results obtained using a rigorous three-dimensional (3D) finite element-based model recently developed by the authors of this paper with those obtained based on these simplifications. The comparison results have shown that both the simplified superstructure models and the newly developed soil reaction curves of the PISA project provide very good results of the OWT natural frequency.*

Keywords: Offshore wind turbines, monopile, natural frequency, superstructure models, PISA, 3D finite element model

## NOMENCLATURE

| | |
|---|---|
| $k_p$ | Initial stiffness of the lateral load-displacement $p-y$ curves |
| $k_m$ | Initial stiffness of the moment-rotation $m-\psi$ curves |
| $k_H$ | Initial stiffness of the shear-displacement spring at pile base |
| $k_M$ | Initial stiffness of the moment-rotation spring at pile base |
| $B$ | Parameter [12] $(= 875)$ |
| $K_0$ | Coefficient of lateral earth pressure |
| $G_0$ | Small-strain shear modulus |
| $\gamma'$ | Submerged unit weight of the soil $KN/m^3$ |
| $\nu$ | Poisson's ratio |
| $p'$ | Mean effective stress |
| $p_{ref}{}'$ | Reference pressure $= 101.3\ kPa$ |

## 1. INTRODUCTION

Nowadays, wind energy sector is evolving worldwide at a very rapid rate. Request for renewable energy is rising and there is a need for increasing the efficiency and design lifetime of offshore wind turbine (OWT) structures. The majority of existing OWTs are installed on monopile foundations [1], with the size of the monopiles increasing as the turbines are moving to more challenging sites (deeper water and weaker soil conditions) and also with the increase of the turbine size.

One of the biggest challenges of the design of multi-megawatt OWTs founded on large-diameter monopiles is that they are dynamically sensitive at the lower frequencies due to their structural slenderness, and the huge concentrated mass located at their tower top. Indeed, the first natural frequency of the overall wind turbine should be carefully adjusted in a very narrow range to be outside the excitation frequencies to avoid resonance. OWTs founded on monopiles are regularly designed as "soft-stiff" structures, where the fundamental natural frequency of the overall wind turbine lies between the exciting frequency corresponding to the rotor frequency (1P) and blade shadowing frequency (3P). Furthermore, DNV [2] suggested that the first natural frequency should not be within 10% of the 1P and 3P ranges. Therefore, accurate and reliable estimate of the

first natural frequency of an OWT is crucial for an effective design.

The determination of the natural frequencies of a monopile-supported OWT is generally performed in literature based on simplifying assumptions related to the soil-foundation interaction and/or the superstructure. An extensive literature review on the different representations of the superstructure and/or soil-foundation interaction of an OWT was performed by the authors in [11] and only a brief description is provided herein. In most previous works [3-5], the superstructure is usually modelled using simplified approaches by employing beam elements for the monopile and the tower and a lumped mass for the rotor-nacelle-assembly (RNA). The simplification of the RNA atop the tower as a point mass is a common engineering practice when calculating the natural frequency. This is because general details on RNA (such as the rotor diameter, the nacelle, the hub and the blades' mass) are easily available and are quite simple to model. Furthermore, the local details of the blades (shape profile, material distribution and strength) are often difficult to find because the aerodynamic profile of the blades is often patented and represents an offshore industry asset. The accuracy of the above-mentioned simplifying assumptions for the OWT steel structure (by employing beam elements for the monopile and the tower and a lumped mass for the RNA) when calculating the natural frequencies of an OWT is thus questionable.

In addition to the simplifying assumptions used for the tower, monopile and RNA, there are other simplifications related to the soil-structure interaction that are used in practice. The standard industry approach for the geotechnical design of monopiles in Europe (as recommended by DNV-GL) is based on the American Petroleum Institute (API) design guidelines [6]. The API method uses the well-known Winkler model [7] where the soil-structure interaction is modelled with empirical soil reaction $\boldsymbol{p-y}$ curves. The traditional API-based $\boldsymbol{p-y}$ curves were calibrated using a limited number of pile tests performed on slender piles with diameters less than 1 m and are now recognized as being unsuitable for large-diameter monopiles used as support for OWTs. Recently, the PISA project provided improved design solutions for laterally loaded large-diameter monopiles tailored for the offshore wind industry (cf. [8] for clayey soil and [9] for sandy soil). The new PISA design model includes a number of different soil reaction components in addition to the lateral soil reaction, $p$, such as a distributed moment, $m$, as well as a base shear $\boldsymbol{H_B}$, and a base moment, $\boldsymbol{M_B}$, as shown in Figure 1. Within, the PISA design model, a new set of depth-dependent calibrated non-linear curves (for each soil reaction component) was developed to be applied in a one-dimensional (1D) finite element model.

This paper aims at checking the ability of (i) the different simplifying assumptions used in literature for the superstructure and (ii) the recently proposed PISA-based soil reaction curves for the soil-foundation interaction model, to reproduce the results of the natural frequencies of a monopile-supported 10 MW DTU OWT installed in sandy or clayey soil as provided by a rigorous three-dimensional (3D) finite element-based model. Notice that the 3D model was recently developed by the authors of this paper making use of Abaqus software. It considers simultaneously both the real geometrical configuration of the OWT superstructure and the 3D soil domain and its interaction with the monopile foundation. Comparison results are presented and discussed.

## 2. MECHANICAL MODEL

The OWT system modelled in this study is consistent with the reference DTU 10 MW three-bladed OWT defined by Bak et al. [10]. Only a brief description of the 3D mechanical model is provided herein. A complete and detailed description of this model may be found in [11].

### 2.1 DTU 10 MW reference wind turbine

The OWT-monopile set-up assumed in this study is representative of the current industry practice and concerns the large 10 MW OWT. An overview of the relevant dimensions is provided in Figure 2, with more details available in [10, 11]. In this paper, the total length of the monopile is chosen as 80 m, in which 25 and 45 m are in the water and seabed, respectively, and another 10 m is added above the mean sea level corresponding to the transition piece.

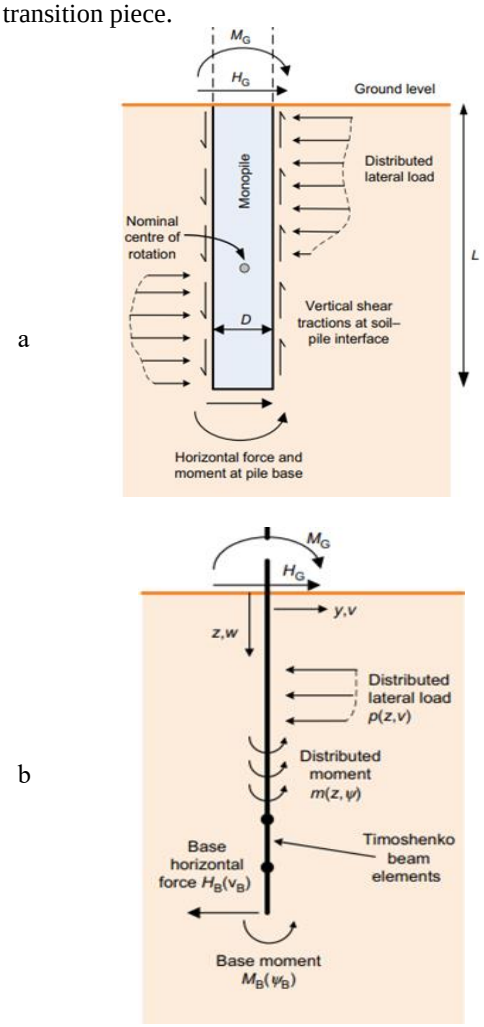


**FIGURE 1:** PISA design model: (a) idealization of the soil reaction components acting on the pile; (b) 1D finite-element implementation of the model showing the soil reactions acting on the pile [8].

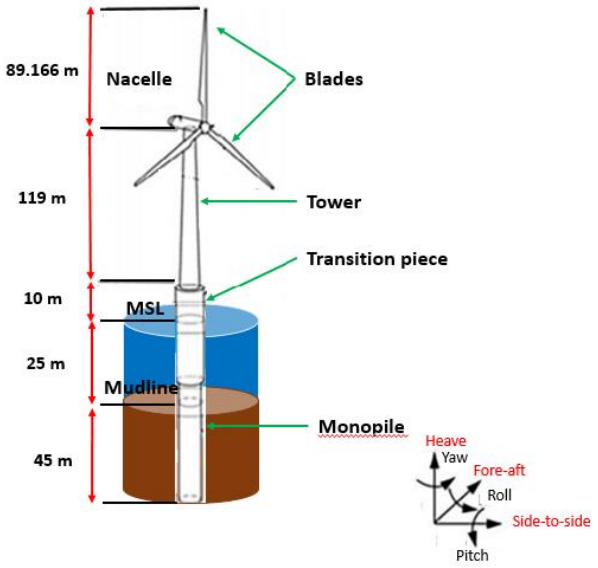


**FIGURE 2:** DTU 10 MW OWT (front view).

### 2.2 3D finite element modelling

The 3D model of the DTU 10 MW OWT used in this work was developed using the finite element (FE) code Abaqus/Standard. Figure 3 shows the developed 3D model of the wind turbine including the soil domain and the corresponding mesh. In this model, the steel structure above the mean sea level (the transition piece and the tower with a decreasing cross-section from the bottom to the top of the tower) was discretized using shell elements. The monopile (in the sea water and in the soil medium) was instead modelled as a 3D hollow cylinder (using solid elements for its discretization) in order to simulate the soil-monopile interaction. The 3D developed model also includes the structural and equipment masses (flanges, paints, welds, bolts and working platforms) as well as the added mass effects due to the surrounding sea water. To consider the influence of the blade's geometry on the calculation of the natural frequency, the blades were explicitly considered in the 3D model. A generalized beam cross-section was defined for every segment of the partitioned blade (51 segments) and for each cross section its corresponding stiffness properties [(i) cross-sectional area, (ii) shear stiffness, (iii) bending stiffness, (iv) extensional and torsional stiffness, (v) and the positions of the mass and shear centers] were assigned. In addition, the nacelle/hub assembly was considered as a lumped mass placed at a reference point whose position coincides with the nacelle center of mass (CM). The CM is located at 2.687 m downwind of the yaw axis and 2.45 m above the yaw bearing [10, 11].

Concerning the soil, a 3D weightless linear elastic domain having a diameter of 20D and a height of 1.7L (see Figure 3) was adopted, where D is the monopile diameter and L is its corresponding embedded depth in the soil. The lateral boundary of the 3D soil domain was restrained in the horizontal direction and the base was fixed in all directions. Concerning the soil-monopile interface, it was modelled using surface to surface master-slave contact pair formulation.

Finally, it is worth mentioning that no damping is considered within the numerical model for the calculation of the natural frequencies.

## 3. NUMERICAL RESULTS

For the estimation of the natural frequencies of the developed 3D model, the structural modal analysis carried out in [11] using Abaqus/Standard is employed herein. Firstly, the natural frequencies and the corresponding vibration modes of the 10 MW DTU OWT installed in loose sand as obtained in [11] are remembered herein. A depth-dependent small-strain Young's modulus profile based on synthetic cone penetration tests (CPTs) data is adopted for the sandy soil (see details in [11]). Secondly, the accuracy of the OWT simplified superstructure models in calculating the natural frequency as obtained in [11] using the depth-dependent small-strain Young modulus profile are provided herein for completeness. Finally, the first natural frequency obtained from the developed 3D model is compared with that provided by the 1D model suggested within the PISA framework.

### 3.1 Results of the 3D FEM-based model

The mass and stiffness distribution for the different components (tower, blades, nacelle and hub) of the 3D developed model was validated by comparing the natural frequencies of the 3D model (with fixed tower base, i.e. without transition piece and monopile) with those given in [10]. A very good agreement was observed and more details may be found in [11]. Table 1 below provides the computed natural frequencies and the corresponding vibration modes of the wind turbine installed in loose sand as obtained from the modal analysis using the developed 3D model. The results show that the major mode shapes of a monopile-supported OWT are the first bending modes of the tower in the side-side and the fore-aft directions shown in Figure 2. The subsequent modes shapes are those of the blade (Modes 3, 4, 5, 6, 7, 9, 11, and 12) and the second bending modes of the tower (Modes 8 and 10).

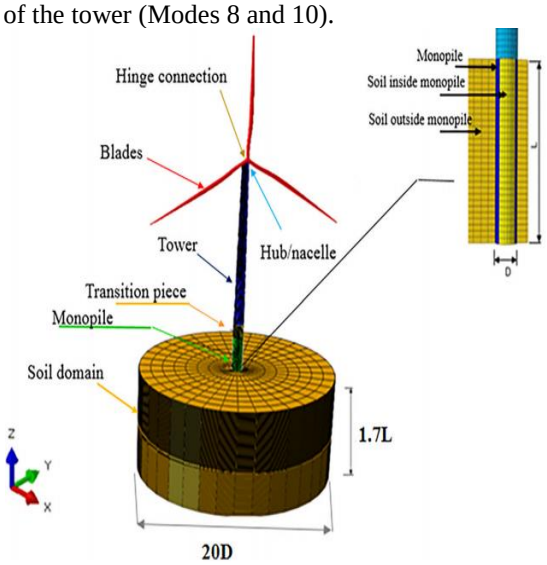


**FIGURE 3:** 3D model of the wind turbine considering the soil-structure interaction.

| Mode | Description | Frequency (Hz) |
|---|---|---|
| 1 | 1st Bending tower, side-side | 0.201 |
| 2 | 1st Bending tower, fore-aft | 0.202 |
| 3 | 1st Blade asymmetric, flapwise yaw | 0.544 |
| 4 | 1st Blade asymmetric, flapwise tilt | 0.589 |
| 5 | 1st Blade collective flap | 0.523 |
| 6 | 1st Blade asymmetric, edgewise 1 | 0.932 |
| 7 | 1st Blade asymmetric, edgewise 2 | 0.941 |
| 8 | 2nd Bending tower, fore-aft | 1.297 |
| 9 | 2nd Blade asymmetric, flapwise Yaw | 1.370 |
| 10 | 2nd Bending tower, side-side | 1.460 |
| 11 | 2nd Blade asymmetric, flapwise tilt | 1.701 |
| 12 | 2nd Blade collective flap | 1.762 |

**TABLE 1:** Natural frequencies of the monopile-supported 10 MW DTU wind turbine installed in a loose sand as computed by the 3D model.

### 3.2 Comparison with the simplified OWT superstructure models

The details of the comparison presented in this section can be found in [11]. Only a brief description is provided herein. In literature, and particularly when calculating the natural frequency of an OWT the nacelle and rotor are rarely modelled in detail. They are poorly included in the analysis as a lumped mass placed atop of the tower [3-5]. Another frequent simplification is the modelling of the tower using beam elements. In order to investigate the suitability of the above-mentioned simplifications, three simplified superstructure models were considered and their results were compared with those of the developed 3D FEM-based model.

The three models labeled 'model 1', 'model 2' and 'model 3" are illustrated in Figure 4. All the three models consider a 3D soil domain as the developed 3D model. Model 1 replaces the RNA by a single lumped mass located at the nacelle CM (i.e. RNA is eccentric to the tower top); however, the tower is still discretized using shell elements. Model 2 consists in replacing (i) the tower by a tapered beam whose diameter and thickness of the different sections are decreasing from the bottom to tower top and (ii) the RNA by a single lumped mass located at the nacelle CM. Model 3 consists in replacing the tower by an equivalent cylindrical beam with a constant diameter of 6.9 m (average tower diameter along its height) and a constant wall thickness of 2.95 cm. The equivalent thickness was computed such that the actual tower mass is maintained [5]. The RNA was considered in this model as a lumped mass located at nacelle CM. Table 2 lists the RNA data used in the three modeling approaches [10].

Figure 5 and Table 3 show a comparison between the values of the first natural frequency obtained by the developed 3D model and the ones obtained by considering the three simplified superstructure models. From Figure 5 and Table 3, one may observe that the approximation made in model 1 by the representation of the RNA as a lumped mass at the nacelle CM tend to overestimate the first natural frequency by only 2.5%. The same result was observed in model 2 when the tower is modelled by beam elements instead of shell elements. Finally, the approximation made upon replacing the tapered tower by an equivalent cylinder with constant wall thickness and diameter (model 3) underestimates the natural frequency by 11.4%. It should be mentioned herein that, although the RNA simplification as a lumped mass tend to overestimate the first natural frequency (Mode 1) by only 2.5% (Model 1), it tends to underestimate the second vibration mode of the tower (Mode 8) by around 11.5%. Also, it is worth to mention that all the simplified superstructure models considered herein give an estimation of the first natural frequency which lies within the allowable frequency range of the 10 MW DTU OWT (i.e. 0.176-0.273 Hz).

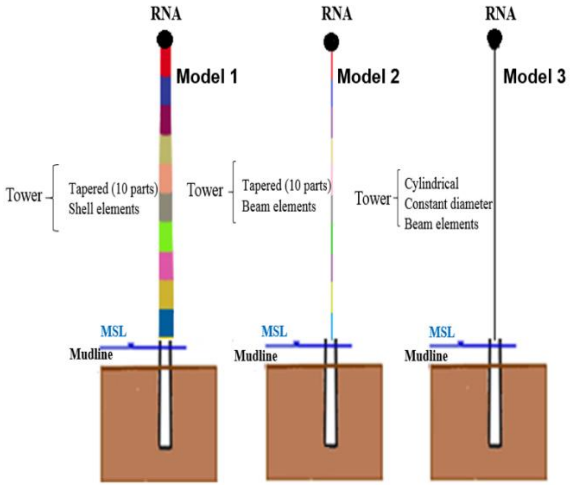


**FIGURE 4:** Simplified superstructure models analyzed in this paper. Only the neutral axis of the beam is shown in models 2 and 3.

| RNA at nacelle center of mass | |
|---|---|
| Lumped mass ($kg$) | 676723 |
| Moment of inertia about x-axis ($kgm^2$) | $1.66\ x\ 10^8$ |
| Moment of inertia about y-axis ($kgm^2$) | $1.27\ x\ 10^8$ |
| Moment of inertia about z-axis ($kgm^2$) | $1.27\ x\ 10^8$ |

**TABLE 2:** Rotor-nacelle-assembly data.

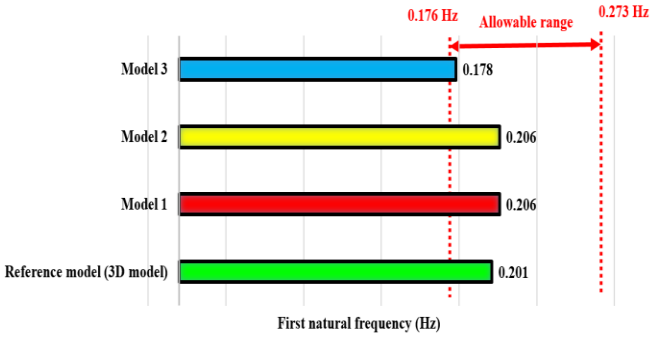


**FIGURE 5:** Predicted first natural frequency for several superstructure models.

| *Superstructure models* | *1st natural frequency (Hz)* | *Deviation (%)* |
|---|---|---|
| 3D model (Reference model) | 0.201 | - |
| Model 1 | 0.206 | 2.5 |
| Model 2 | 0.206 | 2.5 |
| Model 3 | 0.178 | -11.4 |

**TABLE 3:** Deviation between the first natural frequency estimated using the 3D model and the ones estimated using the simplified superstructure models.

### 3.3 Adequacy of the PISA model

The PISA (Pile Soil Analysis) model is an extension of the existing $p-y$ approach in which additional soil reaction components are included to improve the model's performance (Figure 1). The phase I of the PISA research project focused on developping a design methodology for monopiles installed in homogeneous soil conditions.

The aim of this section is to compare the first natural frequency obtained using the PISA design model with the one obtained using the 3D developped model. This comparision allows us to assess the extent to which the PISA design model is a satisfactory surrogate for detailed 3D finite-element analysis when calculating the natural frequency for monopile-supported OWTs in homogeneous soil conditions. It should be noted that the 3D model used in this section is the one presented in section 2.2 (see Figure 3).

The homogeneus soil types that have been used in this paper are those employed in phase I of the PISA project :

(a) a stiff overconsolidated clay known as 'Cowden till' [8] ;
(b) a marine sand known as 'general Dunkirk sand model' with relative density $D_R$ in the range $45\% \leq D_R \leq 90\%$ [9] ;
(c) a soft clay known as 'Bothkennar clay' [12, 13].

As the natural frequency is concerned with very small amplitude vibrations, the deformation of the foundation will be small and consequently, the consideration of the initial foundation stiffness would suffice for this purpose. In this paper, the use of the initial stiffness of the PISA soil reaction curves (when using the PISA model) as well as the small-strain properties of the soil (when using the 3D model) are adopted to perform the linear modal analysis of the OWT in Abaqus. The soil input parameters provided in [13] and shown in Table 4 and Figure 6 are employed herein to obtain the homogeneous ground models for incorporation in the PISA design model and the 3D finite-element analysis. Indeed, Figure 7 shows the profiles of the small-strain shear modulus $G_0$ for the homogeneous soil models employed in the 3D model, and Table 5 gives the depth variation dimensionless initial stiffness functions for the Cowden till [8], Bothkennar clay [12] and Dunkirk sand [9] used in the PISA model.

| | *Cowden till* | *Bothkennar* | *Dunkirk* |
|---|---|---|---|
| $\gamma'$ $(kN/m^3)$ | 11.38 | 6.19 | 10.09 |
| $K_0$ | Variable (see Figure 6) | 0.65 | 0.4 |
| $\nu$ | 0.495 | 0.495 | 0.17 |
| $G_0$ $(kPa)$ | $1100p'$ | $526.8\,p'$ | $\frac{Bp_{ref}'}{0.3+0.7e_0{}^2}\sqrt{\frac{p'}{p_{ref}'}}$ |

**Table 4:** Data employed for the homogeneous ground models for incorporation in the PISA design model and the 3D finite-element analysis [13].

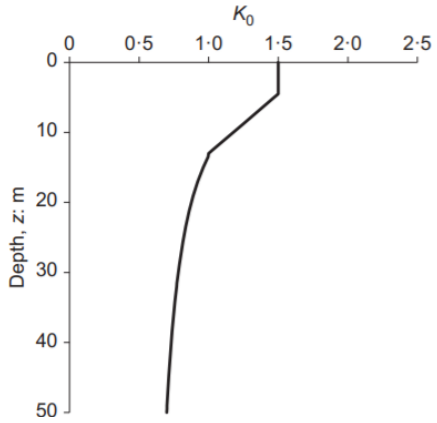


**FIGURE 6:** Depth variation of $K_0$ for the reference homogeneous soil model for Cowden till [8, 13].

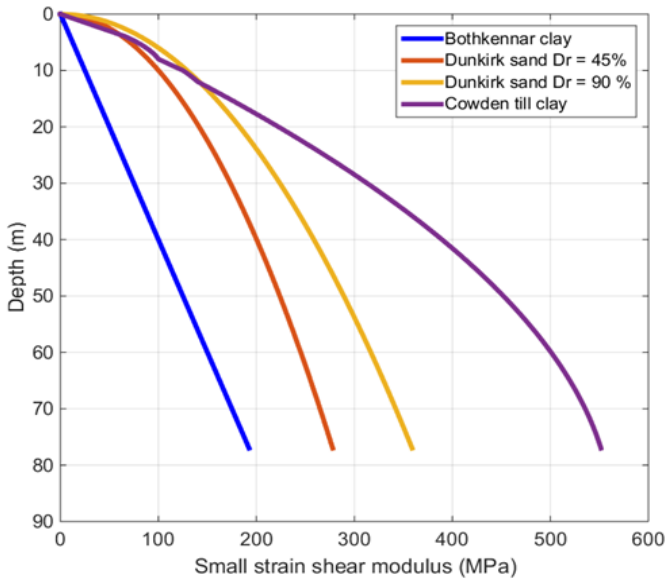


**FIGURE 7:** Small-strain shear modulus $G_0$ profiles implemented in the 3D model based on the equations found in [8, 9, 12, 13].

| Initial stiffness | Cowden till | Bothkennar | Dunkirk |
|---|---|---|---|
| $k_p$ | $10.6 - 1.65\frac{z}{D}$ | $12.05 - 1.547\frac{z}{D}$ | $8.731 - 0.6982D_R - 0.9178\frac{z}{D}$ |
| $k_m$ | $1.42 - 0.09643\frac{z}{D}$ | $1.698 - 0.1576\frac{z}{D}$ | 17 |
| $k_H$ | $2.717 - 0.3575\frac{L}{D}$ | $3.008 - 0.2701\frac{L}{D}$ | $6.505 - 2.985D_R - (0.007969 + 0.4299D_R)\frac{L}{D}$ |
| $k_M$ | $0.2146 - 0.002132\frac{L}{D}$ | $0.3409 - 0.01995\frac{L}{D}$ | 0.3515 |

$D_R$, $L$ and $D$ are the sand relative density and the monopile embedded depth and diameter respectively

**TABLE 5:** depth variation dimensionless initial stiffness functions for the Cowden till [8], Bothkennar clay [12] and Dunkirk sand [9] used in the PISA model.

Concerning the PISA model, a Timoshenko beam representation of the monopile was adopted when implementing this approach in Abaqus. Notice that the soil was modelled by a set of distibuted spring elements equally spaced at 1.0 m interval along the monopile embedded depth (of 45 m) in the following manner :

- ✓ 45 distributed lateral springs [for each lateral direction (x and y direction in Figure 3)] corresponding to the distributed lateral load curves ;
- ✓ 45 distributed rotational springs [for each lateral direction] corresponding to the distributed moment curves ;
- ✓ A translational and rotational spring at the base of the monopile [for each lateral direction] corresponding to the base shear and moment curve respectively.

Also, notice that, the bottom of the monopile is restrained against translation and rotation in the vertical direction.

Figure 8 shows the spring stiffness distribution along the monopile embedded length for the soil conditions considered in this paper. Notice that the values of the lateral springs stiffness in Figure 8a correspond to the initial stiffness of the $p-y$ curves which are obtained by multiplying the dimensionless $k_p$ profile (Table 5) by the small-strain shear modulus profile $G_0$ (Table 4 and Figure 7). Also, the values of the rotational springs stifness shown in Figure 8b correspond to the initial stiffness of the $m-\psi$ curves. They are obtained by multiplying the dimensionless $k_m$ profile (Table 5) by $G_0D^2$ where $D$ is the monopile diameter. Notice that the values of the spring stiffness in Figure 8 are those which are assigned to the distributed springs elements used in the PISA model within Abaqus for the distributed lateral and rotational springs.

Figure 9 shows a comparison between the first natural frequency obtained using the PISA model and the one obtained by the present 3D model for the different soil types considered in this study. To further quantitatively evaluate the accuracy of the proposed PISA model in predicting the natural frequency, the percentage deviations of the estimated natural frequency are calculated (Equation 1) and presented in Table 6 below.

$$Deviation = \frac{f_{PISA}-f_{3D}}{f_{3D}}100\% \quad (1)$$

where $f_{PISA}$ and $f_{3D}$ are the first natural frequency estimated using the PISA and the 3D model respectively.

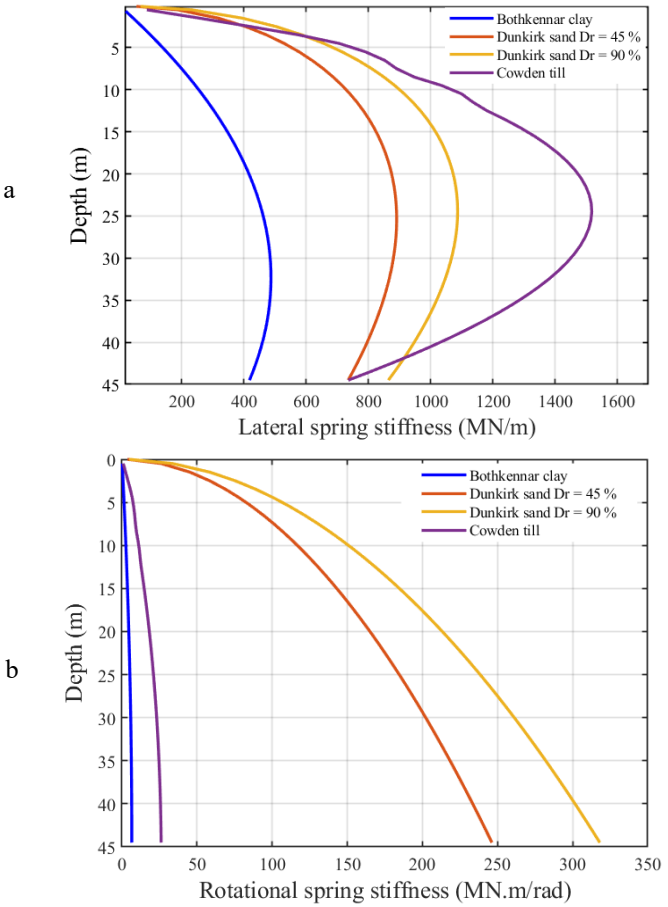


**FIGURE 8:** Spring stiffness distribution along the monopile embedded depth for the PISA model (a) lateral; (b) rotational.

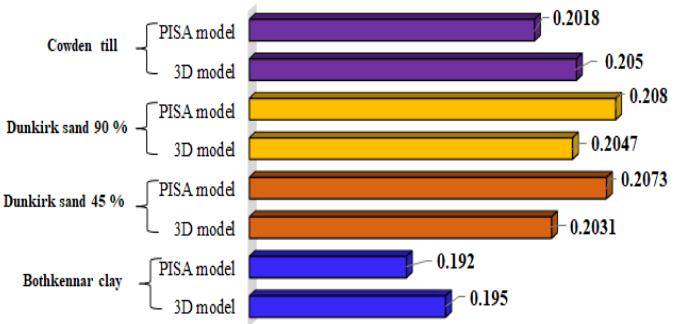


**FIGURE 9:** Predicted first natural frequency of the 10 MW DTU-OWT installed in four different soil conditions using the PISA and the 3D model for the foundation.

From Figure 9 and Table 6, one may observe that the proposed PISA model for the different soil conditions proved to be capable of predicting the first natural frequency of a monopile-supported OWT in parked condition, the percentage deviation being only around 1.5-2%.

A further examination of both figures 7 and 9, allows one to observe that the natural frequency is strongly dependant on the soil stiffness in the zone very close to the mudline. For instance, by comparing the natural frequencies obtained using the 3D model (Figure 9), a decrease of only around 0.15% and 0.9 % in the natural frequency can be found when the soil type changes from a very stiff clayey soil (Cowden) to a dense sand (Dunkirk 90 %) and a loose sand (Dunkirk 45 %) respectively. However, a decrease of 4.9 % is recorded when passing from the very stiff clayey Cowden to the very soft Bothkennar clay. Figure 7 confirms the above mentioned observation. Indeed, although the Cowden posseses a stiffer small-strain shear modulus profile at great depths compared to the other soil types, the Cowden's soil stiffness near the mudline is practically equal to that of Dunkirk and much higher than that of the Bothkennar clay.

| *Soil type* | *Deviation (%)* |
|---|---|
| Cowden till | -1.6 |
| Dunkirk sand $D_R = 90\%$ | 1.6 |
| Dunkirk sand $D_R = 45\%$ | 2.1 |
| Bothkennar clay | -1.5 |

**TABLE 6:** Deviation between the first natural frequency estimated using the 3D model and the ones estimated using the simplified superstructure models

To study the effect of each individual soil reaction curve proposed by the PISA model on the value of the natural frequency, a sensitivity analysis was carried out where the natural frequency was extracted for each soil type using the three following configurations of the PISA model :

C1 : Absence of the distributed moment-rotation springs along the embedded monopile ($k_m$) ;
C2 : Absence of both (i) the distributed moment-rotation springs along the embedded monopile ($k_m$) and (ii) the shear-displacement spring ($k_H$) and the moment-rotation spring ($k_M$) at the pile toe ;
C3 : Absence of the lateral soil-displacement springs, i.e. $p - y$ curves ($k_p$) along the monopile depth.

Figure 10 below gives the first natural frequency obtained using the configurations (C1, C2 and C3) for the different soil conditions studied within the PISA framework . From Figure 10, one may observe that the distributed moment-rotation springs along the monopile embedded length together with the shear-displacement and the moment-rotation springs at the pile base do not have any significant influence on the natural frequency in the case of a monopile installed in a clayey soil (Figure 10a and 10b) and a non-negligible influence (decrease of 4%) in the case of sand (cf. Figure 10c). This result can be explained by the rotational spring stiffness distribution shown in Figure 8b.

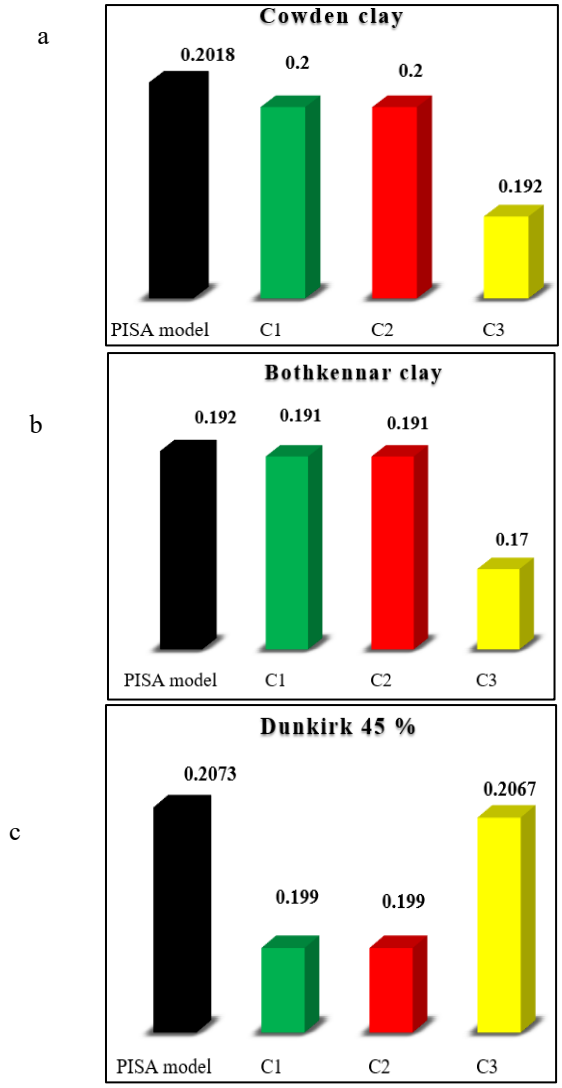


**FIGURE 10:** Predicted first natural frequency of the 10 MW DTU-OWT using the three different configurations C1, C2 and C3 of the PISA soil reaction curves together with the value provided using the four soil reaction curves (a) Cowden clay, (b) Bothkennar clay, and (c) Dunkirk 45%.

Also, notice that the absence of the lateral distributed soil springs (C3) may have a significant impact on the natural frequency in the case of a monopile-supported OWT installed in a clayey soil and a relatively slight influence for the case of monopile installed in Dunkirk sand with 45% relative density, the effect being more important in Bothkennar clay (cf. Figure 10b) where a reduction of 11.5 % is observed. Indeed, the stiffness of the clayey soils (Cowden and Bothkennar) is only governed by the presence of the lateral distributed soil springs (cf. Figure 8) and thus, their absence induces a significant decrease in the value of the fundamental frequency.

## 4. CONCLUSIONS

In this paper, a rigorous 3D model that explicitly considers the geometrical properties of the whole OWT superstructure (blades, tower, and transition piece) and the 3D soil domain together with its interaction with the foundation (see [11]) was used to investigate the suitability of (i) the different simplified superstructure models found in literature and (ii) the recent soil reaction curves proposed within the PISA project for the soil-foundation system, when calculating the natural frequencies of a monopile-supported 10 MW DTU OWT. Based on the obtained numerical results, the following conclusions can be drawn :

1. The representation of the rotor-nacelle-assembly (RNA) by a lumped mass at the nacelle center of mass with the corresponding mass and moment of inertia properties proved to give a very good estimation of the first natural frequency with a deviation of 2.5% only. Moreover, the assumption of modelling the tower with 3D shell elements does not improve the results, and thus the assumption of using a tappered beam with the corresponding properties is sufficient for the natural frequency calculation.
2. The PISA calibrated design model for the homogeneous soil conditions (Cowden, Bothkennar and Dunkirk) resulted in an excellent estimate of the first natural frequency with a deviation of about 1.5-2%.
3. The additional soil reaction components proposed by the PISA project (distributed moment-rotation springs along the monopile embedded length, the shear-displacement spring at pile toe, and the moment-rotation spring at the pile toe) proved not have any significant influence on the natural frequency in the case of a monopile installed in a clayey soil and a considerable influence (decrease of 4%) in the case of sand.

## ACKNOWLEDGEMENTS

This work was carried out within the framework of the WEAMEC, West Atlantic Marine Energy Community, and the funding from the CARENE, Communauté d'Agglomération de la Région Nazairienne et de l'Estuaire.

## REFERENCES

[1] Offshore Wind in Europe, Key trends and statistics 2017.

[2] DNV. *Guidelines for design of wind turbines: Det Norske Veritas*. Wind energy department, Risø National Laboratory (2018).

[3] Adhikari, Sondipon and Bhattacharya, Subhamoy. "Vibrations of wind-turbines considering soil-structure interaction." *Wind and Structures* Vol. 14 No. 2(2011): pp. 85-112.

[4] Jalbi, Saleh and. Bhattacharya, Subhamoy. "A comparision between advanced and simplified methods to predict the natural frequency of offshore wind turbines incorporating soil-structure interaction." *Coastal Structures, Goseberg, Nils & Schlurmann Torsten*: pp. 904-912 Karlsruhe: Bundesanstalt fur Wasserbau2019.

[5] Arany, Laszlo; Bhattacharya, Subhamoy; Adhikari, Sondipon; Hogan, SJ. and Macdonald, John H G. "An analytical model to predict the natural frequency of offshore wind turbines on three-spring flexible foundations using two different beam models." *Soil Dynamics and Earthquake Engineering* Vol. 74(2015): pp. 40-45.

[6] API 2000 Recommended practice for planning, designing and constructing fixed offshore platforms-working stress design – Technical report. American Petroleum Institute.

[7] Winkler, Emil. *"Theory of elasticity and strength of materials."* Prague (1867).

[8] Byrne, Byron; Houlsby, Guy; Harvey, Burd; Gavin, Kenneth; IGOE, David; Jardine, Richard; Martin, Christopher; Mcadam, Ross; Potts, David; Taborda, David; and Zdravkovic, Lidija. "PISA design model for monopiles for offshore wind turbines: application to a stiff glacial clay till." *Géotechnique* Vol. 70 No. 11(2020): pp. 1067-1082. https://doi.org/10.1680/jgeot.20.PISA.009

[9] Harvey, Burd; Taborda, David; Zdravkovic, Lidija; Abadie, Christelle; Byrne, Byron; Houlsby, Guy; Gavin, Kenneth; IGOE, David; Jardine, Richard; Martin, Christopher; Mcadam, Ross; Pedros, Antonio and Potts, David. "PISA design model for monopiles for offshore wind turbines: application to a marine sand." *Géotechnique* Vol. 70 No. 11(2020): pp. 1048-1066. https://doi.org/10.1680/jgeot.18.P.277

[10] Bak, Christian; Zahle, Frederik; Bitsche, Robert; Kim, Taeseong; Yde, Anders; Henriksen, Lars Christian; Natarajan, Anand and Hansen, Morten. "Description of the DTU 10 MW reference wind turbine." DTU Wind Energy Report-I-0092. STU Wind Energy. July 2013. https://rwt.windenergy.dtu.dk/dtu10mw/dtu-10mw-rwt

[11] Alkhoury P, Soubra A-H, Rey V, Aït-Ahmed M. A full three-dimensional model for the estimation of the natural frequencies of an offshore wind turbine in sand. Wind Energy. 2021;24:699–719. https://doi.org/10.1002/we.2598

[12] AWG (Academic Work Group). "Confidential report by the PISA2 Academic Work Group to the PISA2 industrial partners, Rev. E, Document No. 3107410, PISA2 Final Report. Oxford, UK: AWG.

[13] Harvey, Burd; Abadie, Christelle; Byrne, Byron; Houlsby, Guy; Martin, Christopher; Mcadam, Ross; Jardine, Richard; Pedros, Antonio; Potts, David; Taborda, David; Zdravkovic, Lidija and Andeade, Miguel. "Application of the PISA design model to monopiles embedded in layered soils." *Géotechnique* Vol. 70 No. 11(2020): pp. 1030-1047. https://doi.org/10.1680/jgeot.18.P.255

 